

# Contribution of Perfusion in Diffusion Weighted MRI of Orthotopic and Subcutaneous Hepatocellular Carcinoma in Rat

A. Babsky<sup>1</sup>, B. George<sup>1</sup>, and N. Bansal<sup>1</sup>

<sup>1</sup>Radiology and Imaging Sciences, Indiana University, Indianapolis, Indiana, United States

## Introduction

As a quantitative parameter calculated from diffusion weighted (DW) <sup>1</sup>H MRI, apparent diffusion coefficient (ADC) of water may reflect not only diffusion that represents mostly the Brownian motion of the water molecules, but also perfusion in microvessels. It can explain a very wide range of ADC values reported for the liver and hepatocellular carcinoma (HCC) in both animals (1, 2) and humans (3, 4). Previous studies show that for low *b*-values (< 100 s/mm<sup>2</sup>) perfusion dominates diffusion by a factor of 10. However, by using high *b*-values (> 500 s/mm<sup>2</sup>), the influence of perfusion is largely attenuated (5). We compared the perfusion (*b*-values = 0, 10, 20, 30, and 100 s/mm<sup>2</sup>) and diffusion (*b*-values = 220, 350, 600, 1000, and 1600 s/mm<sup>2</sup>) components in the rat liver, and intrahepatic and subcutaneous HCCs. The objective of the study was to evaluate the possible contribution of capillary tissue perfusion and water molecular diffusion in DW <sup>1</sup>H MRI of HCCs located intrahepatically and subcutaneously.

## Methods

DW <sup>1</sup>H MRI was performed on Sprague-Dawley rats. Each animal was imaged 21 days after injection of  $1 \times 10^6$  N1S1 cells into the left liver lobe or on 28 days after injection of  $10 \times 10^6$  cells under the skin on the thigh. MR images were acquired with a Varian 9.4 T, 31-cm horizontal bore system. The water ADC of the HCCs and normal liver tissue was measured with a 63-mm birdcage coil. A multi-slice DW <sup>1</sup>H imaging sequence with the following imaging parameters was used: 1,100 ms repetition time, 21 ms echo time,  $256 \times 128$  data points over a  $80 \times 80$  field of view, 0.5 mm slice thickness, 1.5 mm slice gap, and *b* = 0, 10, 20, 30, 100, 220, 350, 600, 1000, and 1600 s/mm<sup>2</sup>. Respiratory gating was used to minimize the effects of motion on water ADC measurement. Total data collection time for a set of DW <sup>1</sup>H MRI at the ten *b* values was  $\sim 23$  min. DW MRI signal intensity (SI) versus *b* value data were fit to the following biexponential equation for normal liver and intrahepatic HCC:  $SI = A_0[A_f \times e^{-b \times ADC_{fast}} + (1 - A_f) \times e^{-b \times ADC_{slow}}]$ , where  $A_0$  is SI for a *b* = 0 s/mm<sup>2</sup>,  $ADC_{fast}$  and  $ADC_{slow}$  are the fast and slow ADC component which are related to tissue perfusion and random molecular diffusion of water, respectively, and  $A_f$  is the relative contribution of  $ADC_{fast}$  which is related to the relative vascular volume or the fraction of fast moving ADC. A monoexponential equation was used for subcutaneous HCC. PSI-PLOT software was used to analyze  $ADC_{fast}$  and  $ADC_{slow}$  components.

## Results

Transaxial sections of DW <sup>1</sup>H MRI of the rat liver, intrahepatic, and subcutaneous HCC collected using ten *b* values are shown in **Fig. 1**. In intrahepatic and subcutaneous HCCs, <sup>1</sup>H SI with *b* = 0 s/mm<sup>2</sup> was almost 2 and 1.5 times higher, respectively, compared to normal liver (**Fig. 2**). In normal liver and intrahepatic HCC, the curves that describe the DW <sup>1</sup>H SI changes with different *b*-values was biexponential.  $A_f$  in control liver was 0.31, while the values of  $ADC_{fast}$  and  $ADC_{slow}$  were 20.2 and 0.70 mm<sup>2</sup>/s, respectively (**Table 1**). In intrahepatic HCC,  $A_f$  was 0.38, while the value of  $ADC_{fast}$  was lower (9.35 mm<sup>2</sup>/s, *P* = 0.05) and  $ADC_{slow}$  was similar (0.70 mm<sup>2</sup>/s) compared to the healthy liver. In subcutaneous HCC, the curve that describes the DW <sup>1</sup>H SI changes with different *b*-values was monoexponential, reflecting very poor development of the circulatory system (**Fig. 1**). In this HCC model,  $ADC_{slow}$  (0.65 mm<sup>2</sup>/s) did not differ compared to intrahepatic HCC and liver (**Table 1**).

## Discussion

Water ADC measurements in HCC, metastases, and hepatic angiomas are higher than those of hepatic parenchyma (4). These measurements, however, may include a contributory perfusion component, particularly in tissues with a rich vasculature such as intrahepatic HCC. The data presented here shows that  $ADC_{fast}$ , which contributes 38% to the total signal in intrahepatic HCC, is significantly lower compared to the normal liver value. This decrease may be because of restricted perfusion in abnormal tumor microvessels. Respiratory motion may also contribute to  $ADC_{fast}$  because the motion artifact was clearly visible in liver bearing HCC. However, the motion did not affect  $ADC_{slow}$  which was similar to that of subcutaneous HCC that is insensitive to abdominal motion. Thus, simultaneous monitoring of water ADC changes in intrahepatic and subcutaneous HCCs may be useful, but the possibility of location-based physiological and metabolic differences must be recognized. Vascular architecture and thus its response to therapy not only vary among tumor types, but may differ between transplanted and spontaneous tumors (6). These differences may lead to different altering in ADC to chemo-, radio-, or immunotherapy.

## Conclusion

A biexponential model for analysis of non-invasive DW <sup>1</sup>H MRI provides important information about neoplastic transformation in capillary liver tissue perfusion and water molecular diffusion. Recognition of both perfusion and diffusion components of water ADC may be important for monitoring tumor growth and response to therapy of orthotopic and metastatic HCC.

**References:** 1) Yuan et al. *World J Gastroenterol* 2005; 11: 5506-5511. 2) Padhani et al. *Neoplasia* 2009; 11: 102-125. 3) Taouli et al. *Radiology* 2003; 226: 71-78. 4) Colagrande et al. *Radiol Med* 2006; 111: 392-419. 5) Thoeny et al. *Neoplasia* 2005; 7: 779-787. 6) Field et al. *Br J Cancer* 1991; 63: 723-726.

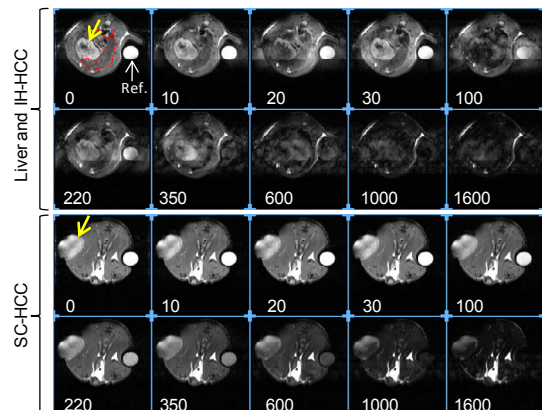


Fig. 1. Representative transaxial slices of DW <sup>1</sup>H MRI of the rat liver, intrahepatic (IH) and subcutaneous (SC) HCC with different *b* values. HCCs are marked by arrow and liver is marked by dotted line. *b*-values are in s/mm<sup>2</sup>. Ref. – reference (0.3 mM NaCl).

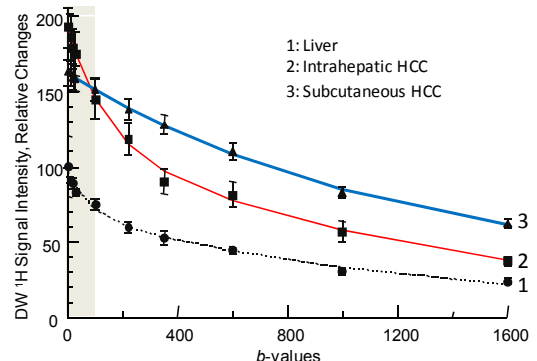


Fig. 2. Perfusion and diffusion component of ADC in the rat liver, intrahepatic and subcutaneous HCCs (mean +/- SEM, *n* = 8). The signal intensity in liver with *b* = 0 s/mm<sup>2</sup> is normalized to 100. Shading indicates the perfusion component area.

Table 1. Fast and slow components of water ADC in the rat liver, intrahepatic (IH) and subcutaneous (SC) HCC.

Parameter	Liver	IH-HCC	SC-HCC
$A_0$	$99 \pm 7$	$193 \pm 13^*$	$163 \pm 9^*$
$A_f$	$0.31 \pm 0.05$	$0.38 \pm 0.05$	0
$ADC_{fast}$	$20.2 \pm 5.3$	$9.35 \pm 1.62^*$	-
$ADC_{slow}$	$0.70 \pm 0.08$	$0.70 \pm 0.09$	$0.65 \pm 0.02$

Note. ADC values are in  $10^{-3}$  mm<sup>2</sup>/s. \* - *P*  $\leq 0.5$  (vs. Liver)